Engineering Conferences International
ECI Digital Archives

The 14th International Conference on Fluidization – From Fundamentals to Products

Refereed Proceedings

2013

# Development of a Novel Concept of Solar Receiver/Thermal Energy Storage System Based on Compartmented Dense Gas Fluidized Beds

R. Chirone
*Istituto di Ricerche sulla Combustione, Italy*

P. Salatino
*Università degli Studi di Napoli Federico II, Italy*

P. Ammendola
*Istituto di Ricerche sulla Combustione, Italy*

R. Solimene
*Istituto di Ricerche sulla Combustione, Italy*

M. Magaldi
*Magaldi Industrie, Italy*

***See next page for additional authors***

**Authors**
R. Chirone, P. Salatino, P. Ammendola, R. Solimene, M. Magaldi, R. Sorrenti, G. De Michele, and F. Donatini

# DEVELOPMENT OF A NOVEL CONCEPT OF SOLAR RECEIVER/THERMAL ENERGY STORAGE SYSTEM BASED ON COMPARTMENTED DENSE GAS FLUIDIZED BEDS

R. Chirone[a], P. Salatino[b]*, P. Ammendola[a], R. Solimene[a], M. Magaldi[c], R. Sorrenti[c], G. De Michele[d], F. Donatini[d]
[a]Istituto di Ricerche sulla Combustione - Consiglio Nazionale delle Ricerche;
P.le V. Tecchio, 80, 80125, Napoli, Italy
[b]Dipartimento di Ingegneria Chimica - Università degli Studi di Napoli Federico II
P.le V. Tecchio, 80, 80125, Napoli, Italy
[c]Magaldi Industrie;
Via Irno, 219, 84135, Salerno, Italy
[d] Magaldi consultant
Via Irno, 219, 84135, Salerno, Italy
*T: +39 081 7682258; F: +39 081 5936936; E: salatino@unina.it

## ABSTRACT
The development of a novel concept of Concentrated Solar Power (CSP) generation system featuring thermal energy storage is addressed. The system is based on a compartmented dense gas fluidized bed. A dynamical model of the system laid the basis for optimizing collection of incident radiative power, heat transfer to the steam cycle, storage of energy as sensible heat of bed solids. It provided the ground for the basic design of a 100kWth demonstration CSP plant.

## INTRODUCTION
Development and deployment of Concentrated Solar Power (CSP) generation is gaining renewed interest. The US Department of Energy has launched the SunShot program [1] targeted at reducing the LCOE from CSP to less than 6cent/kWh. The European Commission has laid the path to CSP development and deployment in the Framework Programmes and in the forthcoming SET plan [2]. A survey by IEA has recently analyzed priorities and opportunities associated with CSP [3], highlighting the key role of integrated thermal energy storage (TES) and fuel-power hybridization for the successful exploitation of concentrated solar power.
The potential of gas-solid fluidized beds (or - more generally - of gas-solid suspensions) as useful components in CSP has been recognized. The use of fluidized solids as alternative to other storage/exchange media, like molten salts, entails the possibility to overcome issues associated with the use of corrosive or environmentally unfriendly fluids and to operate the receiver at much higher temperature (with associated improved overall efficiency of the energy conversion cycle). Fluidized bed solar receivers have been investigated at the proof-of-concept or lab-scale levels [4-12], but full exploitation at the demonstration scale is still missing.
A research consortium has been established by the Magaldi industrial group, the University of Naples and the National Research Council of Italy with the goal of developing a novel concept of solar receiver for CHP (combined heat and power) generation featuring thermal energy storage. The basic concept is the development of a Solar Generation Unit (SGU) consisting of a compartmented dense gas fluidized bed (Fig. 1) optimized so as to accomplish the following three complementary tasks:

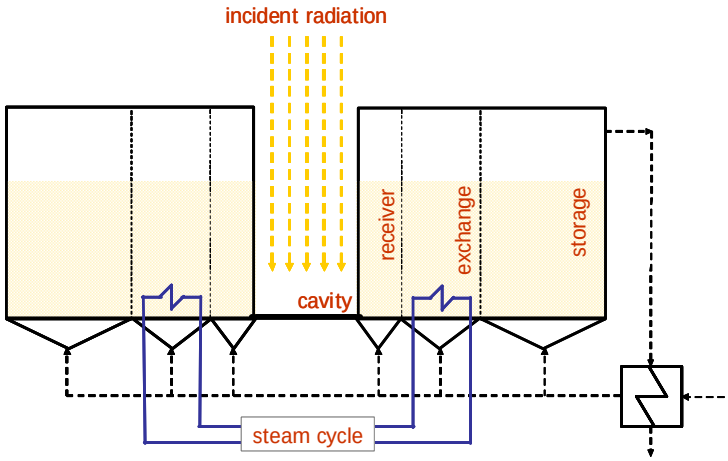


**Fig. 1 –** Conceptual representation of the solar receiver/thermal energy storage system based on compartmented dense gas fluidized beds.

**Collection**: Effective collection of incident solar radiation in a beam-down concentrated solar power arrangement is targeted at limiting re-emission of the incident radiation and at minimizing local overheating at the surface of the receiver exposed to densely concentrated incident radiation.
**Transfer**: The fluidized state of the solids warrants enhanced transfer of the incident power to immersed tube bundles, for optimal integration of the SGU in high-efficiency steam and/or organic Rankine cycles (ORC).
**Storage**: The fluidized solids are exploited as an effective thermal energy storage medium, with the aim of equalizing the inherent time-variability of the incident radiation for stationary CHP generation.

The concept is based on the well established properties of dense fluidized beds of featuring: 1) large bed-to-surface heat transfer coefficients, in the order of several hundreds of $W/m^2K$, which can be tuned by acting on the fluidization parameters; 2) large effective thermal diffusivities, in the order of 0.01-0.1$m^2/s$, associated with convective transfer due to bubble-induced and gulfstream motion of fluidized solids. Both features may be optimized by proper selection of fluidized solids type and size and fluidization regime.
The compartmented solar receiver based on the above principles is outlined in Fig. 1. The present configuration is based on indirect transfer of incident power to the fluidized bed via an irradiated cylindrical cavity immersed in the bed. Alternative designs of the SGU (including direct irradiation of the bed) are being developed.
A dynamical model of the compartmented solar receiver based on the above principles is hereby presented. Computations are aimed at optimizing specific features of the SGU, with a focus on the accomplishment of the three basic tasks (collection, storage and transfer) by a compartmented design of the fluidized bed reactor and a tailored control strategy.
The design of the SGU has been further engineered by defining optimal characteristics of the heliostat field and of the radiation concentration system and by provision of inherent hybridization potential. Several SGUs may be combined in a modular fashion to fit prescribed power generation requirements. A

demonstration 100kWth SGU has been installed and is currently being successfully operated at the Magaldi site in Buccino (SA, Italy).

**THE MODEL**

The mathematical model is based on the scheme of Figure 1. The system consists of a cylindrical cavity where the incident solar radiation is concentrated, a bubbling gas fluidized bed coupled with a steam cycle and an external heat exchanger for partial recovery of the enthalpy of the effluent gas. The windbox is compartmented so as to achieve independent control of fluidization in each of the following zones: 1) the receiver section (R), located nearby the cavity; 2) the exchange section (E), where tube bundles are immersed; 3) the storage section (S), aimed at thermal energy storage as sensible heat of the fluidized solids. The sequential R-E-S arrangement is considered in the present study, though other arrangements might be considered.

The model is based on the following assumptions:

1. The incident solar radiation is uniformly dispersed over the lateral surface of the cavity.
2. The fluidized bed is lumped into three zones (R, E and S), within which the solid and gas phases (in thermal equilibrium) are well stirred. Though there is no physical division between the three zones (e.g. walls), it is assumed that the use of a compartmented windbox provides an effective way to enable independent control of fluidization regimes in each zone.
3. Heat transfer between the i-th and j-th fluidized bed sections is proportional to the temperature difference: $k_{i,j}(T_i - T_j)$. The effective heat transfer coefficient $k_{i,j}$ is given by:

$$k_{i,j} = \rho_s(1-\varepsilon_{mf})cp_s\left(\frac{2H\pi}{\ln\left(\frac{R_j}{R_i}\right)}\right)\alpha_{i,j}$$

where $\rho_s$, $cp_s$, $\varepsilon_{mf}$, $H$, $R_i$ and $R_j$ are solid density and specific heat capacity, the bed voidage at incipient fluidization, the bed height, and the radii of the i-th and j-th fluidized bed sections, respectively. $\alpha_{i,j}$ is the effective thermal diffusivity averaged between the i-th and j-th fluidized bed sections. $\alpha_{i,j}$ is dominated by convection of fluidized solids and has been expressed according to Borodulya et al. [13] as:

$$\alpha_{i,j} = 0.013\left(\frac{D}{H}\right)^{0.5}\left(\frac{U-U_{mf}}{gH}\right)^{-0.15} H\left(U-U_{mf}\right)$$

where $D$, $U_{mf}$, $U$ and $g$ are the transversal fluidized bed length scale, the incipient fluidization and the gas superficial velocities and the acceleration due to gravity, respectively.

4. Heat transfer coefficient, $h_{bed}$, between the fluidized bed and immersed surfaces is calculated according to Molerus et al. [14].
5. Each bed section is virtually insulated with respect to the others and to the cavity when it is not fluidized.
6. The transient behavior of the air-air heat recuperator is neglected by assuming pseudo steady-state.

7. The daily profile of incident solar radiation on the cavity is simulated according to the following law:

$$Q(t)=\begin{cases} Q_{\max}\sin\left(\dfrac{\pi}{\tau_d}t\right) & t\le\tau_d \\ 0 & \tau_d<t\le\tau_d+\tau_n \end{cases}$$

where $\tau_d$ and $\tau_n$ are the duration of the daytime and nighttime phases of the daily cycle, respectively.

Model equations are:

1. Transient energy balance on the cavity:

$$m_C c_C \frac{dT_C}{dt}=\left(1-(1-e_w)F_c\right)Q(t)-S_l\left(h_{bed}(T_C-T_R)+h_{nc}(T_C-T_{amb})+F_c e_w\sigma T_C^4\right)$$

2. Transient energy balances on R, E and S sections of the fluidized bed:

$$\begin{cases} m_R c_{Ps}\dfrac{dT_R}{dt}=h_{bed}(T_C-T_R)S_l-k_{R,E}(T_R-T_E)-S_R U_R\rho_{air}(T_R)c_{Pair}(T_R-T_0) \\ m_E c_{Ps}\dfrac{dT_E}{dt}=k_{R,E}(T_R-T_E)-k_{E,S}(T_E-T_S)-\dfrac{S_f}{\dfrac{1}{h_{bed}}+\dfrac{1}{h_f}}\left(T_E-T_f\right)\Phi(T_E-T_{\min})+ \\ \qquad\qquad -S_E U_E\rho_{air}(T_E)c_{Pair}(T_E-T_0) \\ m_S c_{Ps}\dfrac{dT_S}{dt}=k_{E,S}(T_R-T_E)-S_S U_S\rho_{aria}(T_S)c_{Pair}(T_S-T_0) \end{cases}$$

3. Energy balance at the fluidized bed exhaust:

$$S_R U_R\rho_{air}(T_R)c_{Pair}T_R+S_E U_E\rho_{air}(T_E)c_{Pair}T_E+S_S U_S\rho_{aria}(T_S)c_{Pair}T_S=$$
$$\left(S_R U_R\rho_{air}(T_R)+S_E U_E\rho_{air}(T_E)+S_S U_S\rho_{air}(T_S)\right)c_{Pair}T$$

4. Energy balances on air-air heat recovery exchanger:

$$\begin{cases} \dot{M}c_{Pair}\left(T-T_{out}\right)=\dot{M}c_{Pair}\left(T_0-T_{amb}\right) \\ \dot{M}c_{Pair}\left(T_0-T_{amb}\right)=U_{EX}S_{EX}\left(T-T_0\right) \end{cases}$$

$m_C$, $c_C$, $T_C$, $e_w$, $F_c$, $S_l$ are the mass, specific heat, temperature, emissivity, view factor and area of the lateral surface of the cavity. $h_{nc}$ and $\sigma$ are the heat transfer coefficient due to natural convection in the cavity and the Stefan-Boltzmann constant. $m_i$, $T_i$, $S_i$, $U_i$, are mass, temperature, cross section and fluidization velocity of the i-th fluidized bed section. $\rho_{air}$, $c_{Pair}$ are the density and specific heat of air. $S_f$, $h_f$ are the heat transfer surface and the fluid-side heat transfer coefficient in the exchange section. $T_0$, $T$, $T_{out}$, $T_{amb}$ are the temperatures of the gas at inlet and outlet of the fluidized bed, the temperature of the effluent gas, the ambient temperature. $\dot{M}$ is the mass flow rate of fluidizing gas. $U_{EX}$ and $S_{EX}$ are the overall heat transfer coefficient and transfer surface of air-air heat exchanger. It is noteworthy that the third term at RHS of the balance on the E section expresses the thermal power transferred to the thermodynamic cycle. It is assumed that transfer is stopped when the local bed temperature is smaller than a minimum threshold $T_{min}$. This is considered in the model by multiplying this term by the Heaviside function $\Phi(T_E\text{-}T_{min})$.

Rearranging the equations, the core of the model is a system of four ODEs, solved in the MathCad™ environment by a fourth order Runge–Kutta algorithm with adaptive integration step size.

## RESULTS AND DISCUSSION

Model computations have been illustrated with reference to the set of input variables reported in Table 1. Three cases have been considered:

Case A. A reference case in which the fluidized bed has been operated without partitioning of the fluidizing gas, i.e. the whole bed has been permanently fluidized at the constant and uniform gas superficial velocity of 0.044 m/s.

Case B. A non-controlled compartmented case in which the R, E and S sections have been fluidized independently of each other. The gas superficial velocity has been set at 0.02 m/s in the S section. The gas superficial velocities in the R and E sections have both been set at 0.1 m/s which provide locally optimal values to maximize heat transfer with the cavity and the tube bundle, respectively. Notably, the overall gas flow rate to the bed in Case B is the same as that in Case A.

Case C. A controlled compartmented case, similar to the previous case B, but with the additional implementation of a control strategy aimed at minimizing energy losses based on the following actions:

a. the receiver is fluidized only during the day cycle, it is defluidized at night. This measure ensures minimization of the heat loss from the fluidized bed towards the cavity at night.
b. the storage section S is fluidized only if:

$$\left|T_E - T_S\right| > \Delta T$$

where $\Delta T$ is a control parameter. This measure aims at minimizing loss related to the enthalpy of fluidizing gas leaving the S section, by defluidizing S when fluidization is unnecessary.

**Table 1 -** Model Parameters

| | | |
|---|---|---|
| Cavity | Mass, kg | 200 |
| | Irradiated surface, $m^2$ | 6.3 |
| | Emissivity, - | 0.92 |
| | View Factor, - | 0.125 |
| | $h_{nc}$, $W/m^2K$ | 5 |
| Receiver section | Solids inventory, kg | 2800 |
| Exchanger section | Solids inventory, kg | 3900 |
| Storage section | Solids inventory, kg | 15000 |
| Bed solids (sand) | Density, $kg/m^3$ | 2600 |
| | Sauter mean diameter, μm | 150 |
| | Voidage at incipient fluidization, - | 0.45 |
| Steam cycle | Average $T_f$, K | 623 |
| | $S_f$, $m^2$ | 0.81 |
| | $h_f$, $W/m^2K$ | 2000 |
| | $T_{min}$, K | 723 |
| External heat recuperator | $S_{EX}$, $m^2$ | 34 |
| | $U_{EX}$, $W/m^2K$ | 27 |

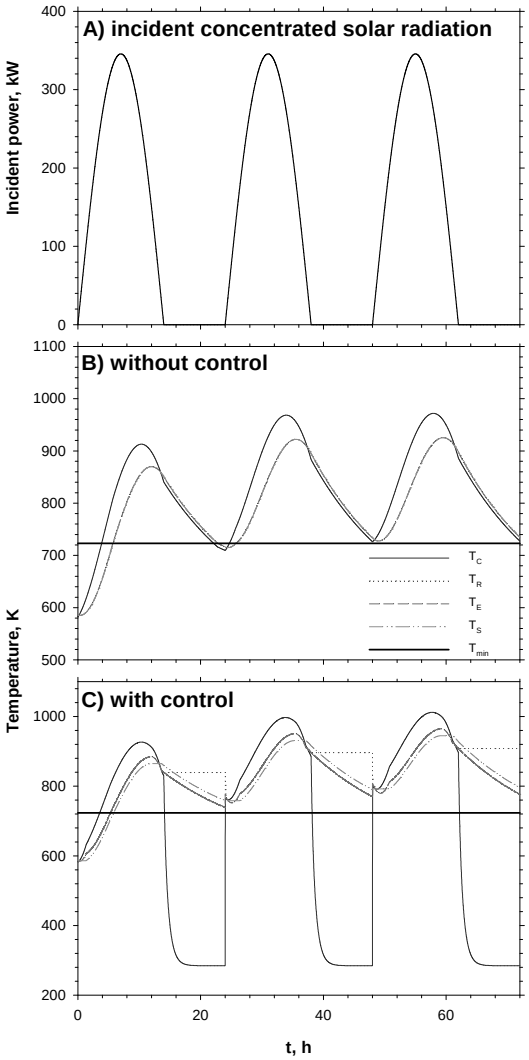


**Fig. 2 –** Model results. A) Time series of the simulated incident radiative power. B-C) time series of the temperature of the cavity and of the fluidized bed sections over repeated cycles. B) computations referred to Case B; C) computations referred to Case C

Results are presented in Figure 2 and in Table 2. Figure 2A reports the incident power profile simulated in the computations. A time-averaged power of 128 kW over a daily cycle was assumed, with $\tau_d$ =14 hr and $\tau_n$ =10 hr. Figures 2B and C report the computed time series of the temperatures of the various sections of the SGU during operation of the unit. Figure 2B refers to the non-controlled Case B computations. Figure 2C corresponds to Case C. An arbitrary initial temperature of 583K has been assumed for all the sections in the simulation. After a few (two-three in Fig. 2) daily cycles during which the system keeps memory of the initial conditions, the unit approaches periodic operation characterized by constant day-averaged parameters.

Analysis of Figure 2B suggests that the temperatures of the three sections of the fluidized bed (R, E and S) are remarkably overlapped with each other. This is a demonstration of the outstanding ability of fluidized beds to equalize solids temperature as a consequence of its very large effective thermal diffusivity. This finding further supports the concept of using fluid beds as effective thermal

**Table 2 -** Results of model computations

| Case | Power, kW | | | | | | Efficiency, - | | |
|---|---|---|---|---|---|---|---|---|---|
| | Incident radiation | Reflected radiation | Fluidizing gas losses | Cavity radiative losses | Cavity natural convection losses | Power to the steam cycle | Cavity | Fluidized bed | Overall |
| A | 128 | 1.28 | 12.4 | 30.8 | 19.6 | 64.2 | 0.60 | 0.84 | 0.50 |
| B | 128 | 1.28 | 12.9 | 22.5 | 17.5 | 74.2 | 0.68 | 0.85 | 0.58 |
| C | 128 | 1.28 | 4.8 | 19.2 | 12.1 | 91.0 | 0.75 | 0.95 | 0.71 |

storage media. The temperature of the cavity exceeds that of the bed by nearly 70K during the active daytime phase of the cycle, to drop below it during the passive nighttime phase. The solids inventory in the bed, and the associated overall heat capacity, are such that the bed temperature never drops below the limit value $T_{min}$, so that the steam cycle is active over the whole 24hr period. Of course this might not hold true if the bed inventory, and in particular the inventory of the S section, is reduced.

Figure 2C highlights the effect on the time-temperature history of the unit of the control strategy implemented according to Case C. The most remarkable feature is that defluidization of the R section during the passive nighttime phase entails rapid cooling down of the cavity and substantial quenching of the R section, with a positive influence on reduction of heat losses to the environment.

The effect of the combination of compartmented operation of the fluidized bed and of the implementation of the control strategy is better appreciated in Table 2 which reports selected day-averaged variables corresponding to long term operation of the unit. Table 2 compares the time-averaged energy balance on the unit for the non-compartmented Case A, for the compartmented uncontrolled Case B and for the compartmented/controlled Case C. The incident power averaged over the 24hr cycle is balanced by: a) thermal losses from the cavity, which in turn include reflection of incident radiation and radiative and natural convection losses; b) losses of sensible heat associated with the effluent gases; c) power transferred to the steam cycle. All the relevant terms in the time-averaged energy balance are reported in Table 2, together with the computed overall thermal efficiency, expressed as the ratio between the power transferred to the steam cycle and the incident radiative power. The overall thermal efficiency equals the product of the cavity efficiency (accounting for cavity losses) and of the fluidized bed efficiency (accounting for losses of sensible heat of the fluidizing gas). These values are also reported in Table 2 to better appreciate the relevant sources of heat losses to the environment.

Comparison of the computed results for Cases A, B and C indicates the extensive improvements that can be accomplished by proper operation of the fluidized bed receiver. Optimizing the local gas superficial velocities in a compartmented bed (Case B) results in a nearly 10kW additional thermal input to the cycle (due to reduced cavity losses) when compared with the non-compartmented Case A. Further improvement is accomplished in Case C by implementing an optimal control strategy: an additional thermal input to the cycle of nearly 16kW is achieved, which results from extensive reduction of losses in the fluidizing gas as well as from the reduction of cavity losses.

## CONCLUSIONS

A novel concept of Concentrated Solar Power (CSP) generation system featuring thermal energy storage has been presented, based on a compartmented dense gas fluidized bed system. A dynamical model of the system has been developed. It has been shown how model computations may be directed to optimize the

operation of the system, by fully exploiting the properties of the dense fluidized bed and the opportunities given by a compartmented arrangement and a tailored control strategy. Moreover, the model has laid the basis for the design of a 100kWth demonstration CSP plant which is currently being successfully operated at the Magaldi site in Buccino (Salerno - Italy).

**ACKNOWLEDGMENTS**

The study is part of the project “PON01_00761: Solare Termodinamico con Accumulo Solido (SOLTESS)” funded by MIUR in the framework of the Program PON Ricerca e Competitività 2007-2013. The support of Mr Gennaro Somma and Mr Antonio Cammarota is gratefully acknowledged.

**REFERENCES**

1. www.solar.energy.gov/sunshot/csp.html
2. Concentrating Solar Power – From research to implementation, European Commission (2007) ISBN 978-92-79-05355-9.
3. Technology Roadmap - Concentrating Solar Power, OECD/IEA, (2010).
4. G. Flamant, D. Hernandez, C. Bonet, J-P. Traverse. Experimental aspects of the thermochemical conversion of solar energy; Decarbonation of CaCO3. Solar Energy, 24 (1980) 385-395.
5. G. Flamant. Theoretical and experimental study of radiant heat transfer in a solar fluidized bed receiver, AIChE Journal, 28 (1982) 529-535.
6. G. Flamant, G. Olalde. High temperature solar gas heating comparison between packed and fluidized bed receivers-I. Solar Energy, 31 (1983) 463-471.
7. I. M. Haddad, M. M. Elsayed. Transient performance of fluidized bed solar receiver at various parametric conditions. Solar and Wind Technology, 5 (1988) 653–659.
8. R. Koenigsdorff, P. Kienzle. Results of and prospects for research on direct-absorption fluidized bed solar receivers. Solar Energy Materials, 24 (1991) 279–283.
9. C. Sasse, G. Ingel. The role of the optical properties of solids in solar direct absorption process. Solar Energy Materials and Solar Cells, 31 (1993) 61-73.
10. J. Werther, R. Koenigsdorff, M. Fischer. Use of Circulating Fluidized beds as solar receivers. Preprints of Annual Meeting Society of Chemical Engineers, Japan Sendai, March 28-30 (1994) pp. 60-61.
11. T. Kodama. High-temperature solar chemistry for converting solar heat to chemical fuels. Progress in Energy and Combustion Science, 29 (2003) 567–597.
12. M. Medrano, A. Gil, I. Martorell, X. Potau, L. F. Cabeza. State of the art on high-temperature thermal energy storage for power generation. Part 2—Case studies. Renewable and Sustainable Energy Reviews, 14 (2010) 56–72.
13. V. A. Borodulya, Y. G. Epanov, Y. S. Teplitskii. Horizontal particle mixing in a free fluidized bed. J. Eng. Phys., 42 (1982) 528.
14. O. Molerus, A. Burschka and S. Dietz. Particle migration at solid surfaces and heat transfer in bubbling fluidized beds--II. Prediction of heat transfer in bubbling fluidized beds. Chemical Engineering Science, 50 (1995) 879-885.